ChemPubSoc Europe

DOI: 10.1002/cphc.201700486

CHEMPHYSCHEM Articles

Special Issue

Investigation on the Interface Modification of TiO_2 Surfaces by Functional Co-Adsorbents for High-Efficiency Dye-Sensitized Solar Cells

Aravind Kumar Chandiran,[a] Shaik M. Zakeeruddin,[a] Robin Humphry-Baker,[a] Mohammad Khaja Nazeeruddin,[a] Michael Grätzel,*[a] and Frédéric Sauvage*[a, b]

The influence of interface modification of sensitized TiO_2 surfaces by co-adsorbents on photovoltaic performance is detailed. We investigated different functional groups of co-adsorbents, such as carboxylic (4-guanidino butyric acid, chenodeoxycholic acid), phosphinic (dineohexyl phosphinic acid), and phosphonic (dodecyl phosphonic acid), to better highlight their influence on the device performance and accurately classify them into de-aggregating agents or agents with both de-aggregating and co-adsorbing properties. By optimizing the type of co-adsorbent and its concentration in the dye solution, we reached an efficiency of 11.0% using 4-guanidino butyric acid or dineohexyl phosphinic acid, compared to 10.6% when the benchmark chenodeoxycholic acid was used. The presence of co-adsorbents on the TiO_2 surface was studied using ATR-FTIR spectroscopy. The role of these co-adsorbents on the band edge shift versus the recombination resistance is discussed.

1. Introduction

Light sensitization of semiconductors dates back to several decades when it became a hot topic for the development of photography.[1] After being recognized that electron-transfer mechanism rules the generation of photocurrent in dye-sensitized semiconductor substrate, the effect of photoconductivity on the mode of dye coverage and the hyper-sensitization were also examined.[2] Discussion on the importance of the dye self-assembly has rapidly become crucial. It is particularly well described in the review of R.C. Nelson as regards of the effectiveness of light absorption by a dye monolayer coverage compared to aggregated units, and, on the underlying effect of photo-excited electron trapping in the latter inducing a loss in value of photovoltage.[3] The concept of hyper-sensitization involves the co-adsorption of molecules having a high electron affinity along with the dye sensitizer to enhance the dark resistivity.[2b,c,4] Since the first ever successful advent of sensitization technology in photovoltaics in 1991, later referred as dye sensitized solar cells (DSSC), several studies involving the formerly mentioned concepts are done to improve the power conversion efficiency of the device. The heart of DSSC lies in a Ru^{II} polypyridyl complex sensitizing anatase TiO_2 nanoparticles deposited onto a fluorine-doped tin oxide (FTO) transparent conducting glass. When exposed to incident illumination, an electron from the dye is promoted from highest occupied to unoccupied energy levels, before to get injected into the conduction band of TiO_2 and collected towards the external circuit. The oxidized dye is regenerated by a hole donation from the dye to iodide (or electron donation from iodide to dye) in the electrolyte (considering iodine/iodide redox mediator). The galvanic chain is looped at the Pt counter electrode from which the external flow of electrons reacts with iodine to reform the original iodide in the electrolyte.[5] Quantitative quantum yield for photon-to-electron conversion in DSSC faces several hurdles. One major is the dye excited state quenching promoted by aggregated units and the electron back transfer to the oxidized form of the redox mediator.[4c,5b,d] To address these important issues, which govern the charge separation and the collection efficiency, respectively, a functional co-adsorbent/de-aggregating agent is basically introduced into the dye solution.[5c,d,6] There are mainly based on carboxylic, phosphinic or phosphonic acid functional groups combined to an amphiphilic alkyl tail which affords to brake aggregated dyes in solution and sometimes to get co-adsorbed onto TiO_2 between dye molecules. The most common molecule associated to Ru^{II} polypyridil complexes and most organic dyes is the chenodeoxycholic acid.[7] Guanidinoalkyl carboxy, alkyl phosphonic and phosphinic acids have also grasp interest to replace the so-called cheno depending on the type of dyes utilized. These additives have the potentialities to improve the open-circuit voltage (V_{OC}) of the device without sacrificing the short-circuit density (J_{SC}). There can also influence the position in energy and

[a] Dr. A. K. Chandiran, Dr. S. M. Zakeeruddin, Dr. R. Humphry-Baker, Prof. M. K. Nazeeruddin, Prof. M. Grätzel, Dr. F. Sauvage
Laboratory of Photonics and Interfaces
Institute of Chemical Sciences and Engineering
Swiss Federal Institute of Technology, EPFL
Station 6, CH-1015, Lausanne (Switzerland)
E-mail: michael.graetzel@epfl.ch

[b] Dr. F. Sauvage
Laboratoire de Réactivité et Chimie des Solides
Université de Picardie Jules Verne, CNRS UMR 7314
33 rue Saint Leu, 80039 Amiens (France)
E-mail: frederic.sauvage@u-picardie.fr

Supporting Information for this article can be found under: https://doi.org/10.1002/cphc.201700486.

An invited contribution to a Special Issue on Physical Chemistry in France

distribution of localized intra-band gap states, dye loading and stability of the device under accelerated ageing conditions (eg. IEC61646) by hampering harmful side reactions between bare TiO_2 and electrolyte.[5c,d,6] However, although reported to be beneficial in most cases, the frontier of the role played by these additives, namely co-adsorbant and/or de-aggregating agent, remains reasonably not clearly defined.

In this work, we have selected one of the best performing and most stable Ru^{II} bipyridyl complex, namely C106, to clarify the effect of various de-aggregating/ co-adsorbent agents with different chemical nature. The objectives are to better highlight the role played by these molecules into practical devices (ie. de-aggreagating vs. co-adsorbing) and to discuss their effects on the photovoltaic performances of C106 dye (ie. power conversion efficiency, traps energy and distribution, recombination dynamic with tri-iodide).

2. Results and Discussions

The (*J-V*) characteristics were measured at AM 1.5 global sun conditions (100 mW cm^{-2}). The devices were assembled using a volatile acetonitrile-based electrolyte with tri-iodide/iodide redox couple. The reference cell, sensitized with C106, exhibits J_{SC}, V_{OC} and the fill factor (ff.) values of 19.3 mA cm^{-2}, 733.7 mV and 74.7 %, respectively. This leads to a power conversion efficiency (PCE) of 10.6 %.

The photoanodes were stained in C106 dye solution containing various concentrations of different co-adsorbents ranging from 6:1 to 1:2 dye to co-adsorbent (D:C) ratio (Table 1 a–d). When using the carboxylic-based GBA zwitterion, it is remarkable to notice that even at a low concentration of one-sixth of its molar concentration in dye solution the J_{SC} is increasing to 20 mA cm^{-2} before to drop gradually on further addition until 17.2 mA cm^{-2} for 0.5:1 ratio. A similar increase of J_{SC} to 19.6 mA cm^{-2} is experienced at a low concentration of cheno before it decreases more marginally to 19.0 mA cm^{-2} at greater concentration, and, with dinhop a maximum of 20.1 mA cm^{-2} is reached at 2:1 ratio before it also slightly declines. By contrast, the incorporation of DPA into the dye solution, the latter bearing a strong binding phosphonic unit, this systematically induces a constant losses of photocurrent while increasing its concentration. It shows no real amelioration of the conversion performances in conjunction with such an efficient ruthenium dye.

The type and concentration of additive in the dye solution influences the cell photovoltage in some circumstances. Only a difference is observed when a relative high concentration of such additive is incorporated into the dye solution. This is the case for GBA when its concentration is same or greater than the dye (from 734 to 763 and 771 mV). Such an improvement is also observed, but to a lower extent, for DINHOP at 0.5:1 ratio (746 mV) and for the DPA for which a photovoltage of 744 mV is attained for concentrations equal and greater than 2:1 ratio. Interestingly, no real effect was found in the case of the cheno regardless of its concentration. The highest photovoltage, namely 771 mV, has been obtained with GBA at D:C ratio of 0.5:1.

Table 1. a) Photovoltaic properties of DSSCs stained with a C106 solution containing guanidino butyric acid co-adsorbents at different concentrations.

C106/GBA ratio	J_{SC} [mA cm^{-2}]	V_{OC} [mV]	FF [%]	PCE [%]
1:0	19.3	734	74.7	10.6
6:1	20.0	738	73.6	11.0
4:1	19.1	735	75.8	10.7
2:1	18.9	734	75.3	10.6
1:1	18.2	763	75.5	10.6
0.5:1	17.2	771	75.2	10.0

b) Photovoltaic properties of DSSCs stained with a C106 solution containing chenodeoxycholic acid co-adsorbent at different concentrations.

C106/Cheno ratio	J_{SC} [mA cm^{-2}]	V_{OC} [mV]	FF [%]	PCE [%]
1:0	19.3	734	74.7	10.6
6:1	19.4	727	72.5	10.2
4:1	19.6	728	74.7	10.7
2:1	19.1	734	75.9	10.7
1:1	19.1	732	74.8	10.6
0.5:1	19.0	735	76.4	10.8

c) Photovoltaic properties of DSSCs stained with a C106 solution containing dineohexyl phosphinic acid co-adsorbent at different concentrations.

C106/Dinhop ratio	J_{SC} [mA cm^{-2}]	V_{OC} [mV]	FF [%]	PCE [%]
1:0	19.3	734	74.7	10.6
6:1	19.2	724	74.9	10.4
4:1	19.2	729	76.0	10.6
2:1	20.1	736	74.9	11.0
1:1	19.9	728	74.4	10.7
0.5:1	19.5	746	75.7	11.0

d) Photovoltaic properties of DSSCs stained with a C106 solution containing dodecyl phosphonic acid co-adsorbent at different concentrations.

C106/DPA ratio	J_{SC} [mA cm^{-2}]	V_{OC} [mV]	FF [%]	PCE [%]
1:0	19.3	734	74.7	10.6
6:1	19.0	733	75.8	10.7
4:1	18.4	734	75.0	10.3
2:1	17.9	744	76.6	10.3
1:1	17.7	743	75.5	10.0
0.5:1	16.8	743	73.1	9.2

We consider that such a beneficial effect of GBA to enhance the photovoltage stems from the carboxylate form of the molecule. Indeed, as shown in Table S1, the related protonated GBA leading to a carboxylic acid function does contribute neither to any photocurrent nor to photovoltage improvement regardless of its concentration into the dye solution. It even induces a constant decrease of photocurrent from 19.3 mA cm^{-2} to 18.0 mA cm^{-2} at 0.5:1 ratio leading to a decrease in power conversion efficiency from 10.6 to 10.1 %. A similar trend is observed for DPA.TBA for which the phosphonic acid function is deprotonated by one equivalent of tetrabutylammonium hydroxide (Table S2). The best power conversion efficiency of 11.0 % is achieved with GBA (at 6:1 D:C ratio). This performance enhancement is credited to a higher photocurrent compared to the reference cell. As similarly to this carboxy-based additives, the utilization of stronger binding unit, namely the phosphinic acid of the dinhop, can also bring the device performance to a level of 11.0 % either by introducing 2:1 ratio to improve the photocurrent without modifying the cell photovoltage or alternatively using 0.5:1 ratio for which in

this case the photovoltage is improved without scarifying the photocurrent in comparison to the reference cell (Table 1 c). To resume, we can estimate that, when having chosen the correct additive, this latter can play two distinct roles depending on their relative concentration: de-aggregation at low a low concentration and de-aggreagation + co-adsorbant greater than a threshold concentration. This threshold value, besides depending on the type of additive and its anchoring group, is function of the solvent, type and number of anchoring group, its structure etc.

The (*J-V*) curves for the best performing DSSCs are gathered in Figure 1 and compared to the reference device free of any additive. The corresponding incident-photon-to-electron conversion efficiency (IPCE) curves are reported in Figure 2. Broad

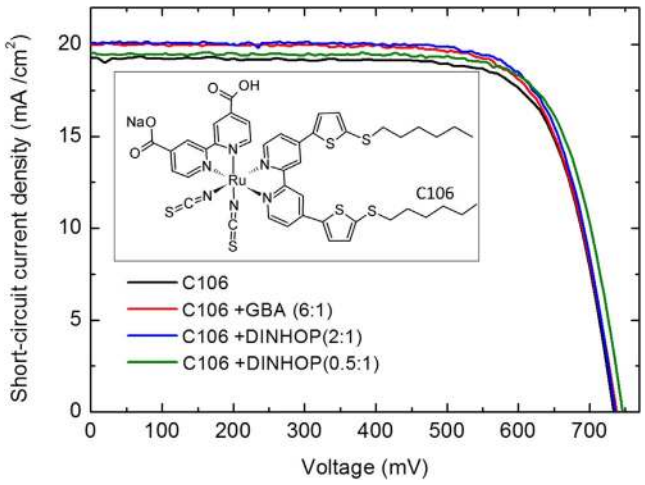

Figure 1. The (*J-V*) curves of cells sensitized with reference C106 and best-performing co-adsorbent-modified GBA and DINHOP cells. The C106 dye structure is shown in the inset.

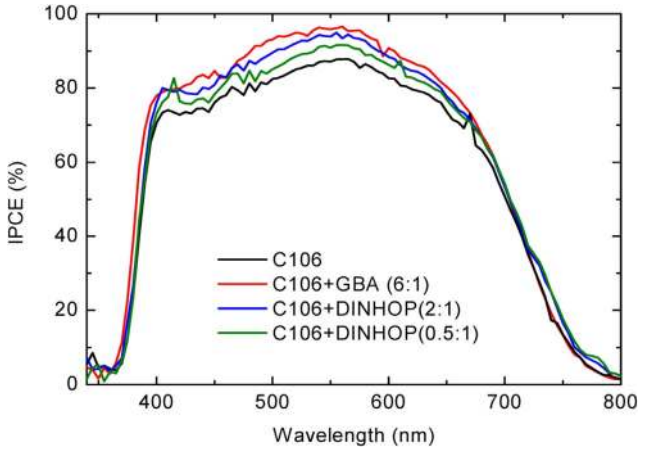

Figure 2. Spectrum of incident-photon-to-electron conversion efficiency as a function of wavelength for the reference C106 and the best-performing co-adsorbent-modified GBA and DINHOP cells.

conversion from 400− to 700 + nm is obtained as a result from the nearly panchromatic absorption of the MLCT (Metal-to-Ligand-Charge-Transfer) band of C106 dye. Without additive, an IPCE maximum of 88% is attained at 550 nm and the tail of conversion reaches over 750 nm. When dinhop or GBA is introduced, the maximum of IPCE increases to 95% and 96% at 550 nm, respectively. This is in good agreement with the greater photocurrent at short-circuit measured under illumination and the integrated action spectra correlates with the value of photocurrent measured at short-circuit by the sun simulator setup. Such a high value of IPCE indicates a quantitative conversion of photons at this wavelength considering the optical losses induced by the NSG10 FTO-glass (i.e. glass absorption and light reflection). Looking carefully to the two tails of IPCE, we can notice that the use of GBA improves slightly the blue conversion by ca. few nm without having any consequences on the red part. By contrast the dinhop enables slightly red-shifting the conversion without having any incidence on the blue part when compared to the reference and GBA (Figure 2). We can hypothesize that the dye geometry when anchored on TiO_2 is affected by the presence or not of the original additive and may also reflect some degree of different dye aggregation level. A similar observation has been discussed in one of our previous work related to the effect of sensitizing temperatures modifying the dye geometry on TiO_2 on the one hand and how its impacts on the dye loading and charge recombination dynamic on the other hand.[8]

Depending on the type of ending group in the additive and the relative concentration to the dye, this latter can become a co-adsorbant on TiO_2 in complement to its primary function of dye de-aggregating agent. To decipher on these two functionalities, we first determined the dye loading on a 9 μm thick photo-anode for the different type of additives and for their relative concentration into the dye solution. For this, the dye loading was estimated by considering the intensity of the dye MLCT absorption band after desorbing the dye from TiO_2 in an alkaline TBA.OH-based DMF solution. For the reference cell, that is, sensitized without any additive into the dye solution, the amount of dye anchored onto the photoanode's surface is 8.6×10^{-8} mol cm^{-2}. Interestingly, the dye loading can be drastically modified depending on the type of additive and its concentration (Table 2). In the case of the zwitterion GBA, its introduction into the dye solution has no noticeable impact on the dye loading regardless of its concentration. Therefore, one can estimate that either GBA does not anchor onto the surface of TiO_2 or alternatively it anchors between the dye molecules without affecting the molecular dye packing. This is noticeably different for the other additives. For instance, with the cheno, the additive the most utilized in association with ruthenium complexes, increasing its concentration induces a slight gradual decreases of dye loading from 8.6 to 8.0×10^{-8} mol cm^{-2} for 0.5:1 D:C ratio. This represents a loss of dyes of ca. 7%. A similar but more marked diminishing trend is also experienced for the phosphinic-based dinhop additive and for the phosphonic acid DPA. However, the stronger binding character of these anchoring groups leads to a more noticeable lowering in dye loading, from 8.6 to 7.4×10^{-8} mol cm^{-2} for the dinhop (14% loss) and even to 3.7×10^{-8} mol cm^{-2} for DPA at a D/C ratio of 0.5:1 (57% loss). This important drop of dye loading when DPA is employed is not totally astonishing since the stronger bind-

Table 2. Amount of dye on a 9 μm thick transparent TiO_2 film for different functional co-adsorbents over a wide range of dye-to-coadsorbant ratios.

	0.5:1 [10^{-8} mol cm^{-2}]	1:1 [10^{-8} mol cm^{-2}]	2:1 [10^{-8} mol cm^{-2}]	4:1 [10^{-8} mol cm^{-2}]	6:1 [10^{-8} mol cm^{-2}]
GBA	8.8	8.7	8.6	8.7	8.6
Cheno	8.0	8.1	8.2	8.4	8.7
Dinhop	7.4	7.6	7.7	8.3	8.5
DPA	3.7	4.3	5.1	6.0	7.3

ing and faster attachment of phosphonic acid group to the surface of TiO_2 than the dye. On the other hand, it can also stem from the bendable amphiphilic C106 alkyl chain which may hamper dye adsorption or facilitate the dye displacement by shielding the adsorption sites of the dye onto TiO_2 surface. This aforementioned hypothesis is further supported by the analysis of the surface chemistry of the sensitized TiO_2 by FT-IR spectroscopy in reflected mode using the ATR technique (Attenuated Total Reflectance). Nevertheless, although almost 60% of less dye on the surface, it is interesting to underline that the photocurrent produced remains at a relatively high value. This means the dye molecule present still absorb and convert a significant fraction of light. Such effect has already been observed in the literature by Graetzel, Frank and co-workers when using a closely related cheno molecule, namely the tetrabutylammonium chenodeoxycholate (TBACDC).[6a] This has been attributed to a reduction of dye self-quenching by the aggregates and to a more efficient electron injection.

The FTIR spectra of the reference sensitized C106 dye on TiO_2 is shown in Figure 3a. It gives the spectroscopic fingerprint of the dye when anchored from 1000 to 3200 cm^{-1} wavenumbers. The sharp strong band at 2101 cm^{-1} corresponds to the C≡N stretching mode of the monodentate thiocyanate donor groups that bound to the ruthenium metal center.[8] The aromatic modes of the bipyridine are given by the sharp bands at 1541 cm^{-1}, 1435 cm^{-1}, 1234 cm^{-1} and 1020 cm^{-1} corresponding to in plane stretching modes of C=C and C=N bonds. The bands at 1608 cm^{-1} and 1386 cm^{-1} are attributed to the asymmetric and symmetric stretching modes of the carboxylate group on the bipyridine ligands. The absence of the two closely related acid bands supports the bidentate mode of anchoring of C106 onto TiO_2 surface. The bands at 2927 cm^{-1} and 2856 cm^{-1} are ascribed to the C-H asymmetric and symmetric stretching modes of CH_2 whereas the band at 2957 cm^{-1} corresponds to the C-H stretching mode of the terminal CH_3 in the

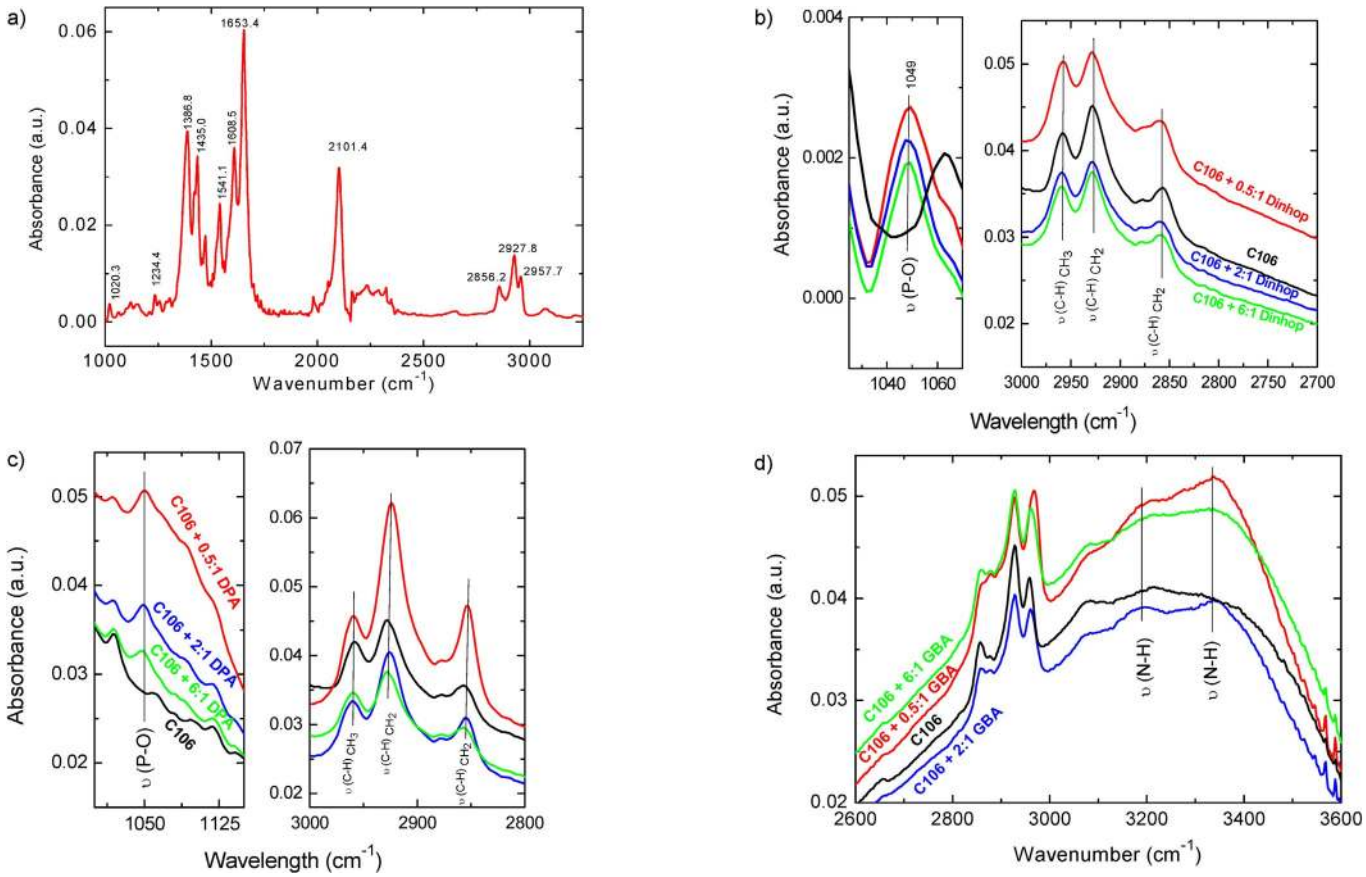

Figure 3. a) ATR-FTIR absorption spectrum of C106 dye sensitized on the titania surface. b) P-O stretching peaks (left) and C-H stretching bands of CH_2 and CH_3 (right) for C106 co-sensitized with dinhop, (c) P-O stretching peaks (left) and C-H stretching bands of CH_2 and CH_3 (right) for C106 co-sensitized with DPA, (d) N-H stretching peaks of C106 co-sensitized with GBA.

hydrophobic alkyl chain of the dye. An additional strong band is observed at 1653 cm^{-1} which does not correspond to the dye. This latter is attributed to the C=O stretching of DMF used originally in the dye solution composition (10% of DMF) to increase the dye solubility compared to a pure mixture of tert-butanol/ acetonitrile mixture.[6e]

We also analyzed the surface of the corresponding photoanodes stained into a dye solution containing the additives at different concentration. This aspect, rarely tackled in the literature so far, sheds the light on one of the real role hold by such additives beside its de-aggregating functionality. For the dinhop, the different spectra are gathered in Figure 3b as a function of D:C ratio. Regardless of dinhop concentration, the spectra shows the appearance of an additional strong and sharp band at 1049 cm^{-1} ascribed to the C-O vibration mode in the P-*O*-C unit of the dinhop.[8] Another feature clearly visible in Figure 3b is a modification in the band intensity ratio of the C-H stretching between those from CH_3 at 2957 cm^{-1} and those from CH_2 at 2927 cm^{-1}, this latter is increasing when the dinhop is introduced. This is an additional hint supporting the presence of dinhop adsorbed on the surface of TiO_2 along the dye since the dinhop structure is richer in CH_3 than the dye, six per formula unit compared to only two for the dye. Similarly to the dinhop, the series of spectra recorded for DPA show the occurrence of C-O vibration mode at 1047 cm^{-1} originating from P-*O*-C group of the phosphonic acid function (Figure 3c). There is also a decrease in the $\upsilon_{(C\text{-}H)CH3}/\upsilon_{(C\text{-}H)CH2}$ ratio which in turn can be explained by the richness in CH_2 of the DPA compared to the dye. These two observations gives therefore credit to the conclusion that DPA is a co-adsorbant along with the dye; a result again not surprising since the strong binding character of the phosphonic acid function to the acidic surface of TiO_2 (and closely related metal oxide materials). Based on the fact that the dye loading decreases when increasing the concentration of dinhop and more markedly for DPA, this suggests that such family of co-adsorbant tends to replace the dye on its binding site rather than/or in addition to a filling of the free-space between the dye molecules.

This falls again in contrast with GBA and the cheno. Indeed, the presence at the surface of the GBA is verified by the spectroscopic fingerprint of the broad N-H asymmetric stretching bands at 3336.6 and 3211.2 cm^{-1}, corresponding to asymmetric and stretching modes, respectively (Figure 3d).[6h] Whereas the dye loading is not affected regardless of its concentration, this seems to support that GBA fills the dye interspace with likely a weak electrostatic interaction with TiO_2 owing to its zwitterion form hampering a strong binding. The case of cheno is more complicated. Indeed, despite several attempts to subtract the reference C106 spectra from cheno modified samples, we have no clear evidence that this latter works as a co-adsorbent, at least for this range of concentration and for such family of dyes. Indeed, cheno has been reported to be adsorbed on the surface in the case of organic dyes such as the squaraine and for a relatively high concentration into the dye solution (i.e. $\geq$10 mmol L^{-1}; D/C $\geq$1:10).[9] It absorbs onto the surface of TiO_2 in absence of dyes (Figure S1). It seems based on our results that the cheno does not absorb onto TiO_2's surface along the dye or to a very low extent. This most probably tends to support that some of the dyes are aggregated at the surface into the reference cell, and that the use of cheno assists mainly to the process of dye deaggregation.

Because the dye geometry and loading is affected by the presence of these additives (DPA, dinhop and GBA) at the surface of TiO_2 and that small organic molecules can exhibit high electrostatic polarizability properties, one can expect noticeable consequences in the distribution and energy of the surface trapping states located below TiO_2's conduction band. In Figure 4, we show the energy as a function of the number of

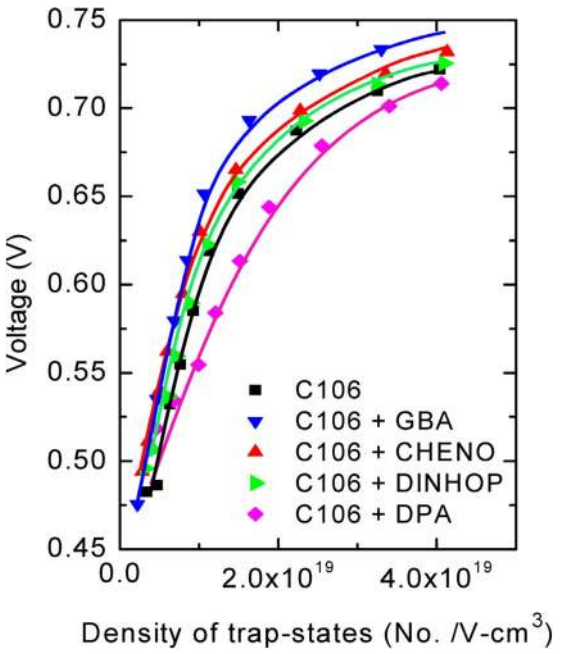

Figure 4. Distribution of density of electron trapping states on TiO_2 for reference C106 and different co-sensitized films.

trap states for the different co-adsorbent at same ratio into the dye solution (1:1). This was determined by charge extraction technique employing different level of illumination from 1.5 to 0.16 sun.[7d,10] It shows that the stronger the binding, the more the traps are downshifted. Such an effect is the consequence of the modification in the interfacial electrostatic dipole moment moving up or down the traps when a molecule is anchored onto nanocrystals of TiO_2.[11] Compared to the reference C106 without any additive into the dye solution, the zwitterion GBA contributes to the most positive shift by ca. 40 mV. Less difference is observed with the cheno (ca. +28 mV) and the dinhop (ca. +8 mV). Such a shift with the cheno stems likely from the different dye loading at the surface and from a different dye geometry/ aggregation level upon the surface as the cheno is not going to the surface or to a very low extent. If a low fraction of cheno goes to the surface, the attachment proceeds through the acid with a loss of proton. The lower energy of the traps with the acid (cheno) compared to the carboxylate (GBA) is consistent with what it is typically experienced with the effect of protonation of the dye anchoring

groups.[12] In the case of the DPA, as aforementioned, this later strongly attached to the surface induces a noticeable downshift in energy of the trap states by ca. 48 mV. One possible explanation to account for this downshift is its higher proton content in the anchoring group. Note that the distribution of the surface traps is also modified by contrast to the cheno, GBA, dinhop and the reference device for which the trap distribution is rather similar.

To have a reasonable comparison in the variation of the open-circuit photovoltage (V_{OC}) for the different additives, one has to compare this photovoltaic parameter at a given charge density. After the charges are injected into the conduction band of titania, the ability of the co-adsorbent and the dye to impede these photo-generated electrons to get intercepted by tri-iodide will determine the open circuit voltage. Owing to technological limitations, the quantification of the effective amount of photo-generated electrons in the conduction band at open-circuit is difficult. To bypass this issue, an indirect method of quantification has been developed considering the fact that at short-circuit the recombination is negligible. Consequently, the short-circuit current density J_{SC} can be considered equal to the overall photo-generated electrons.[10] Figure 5

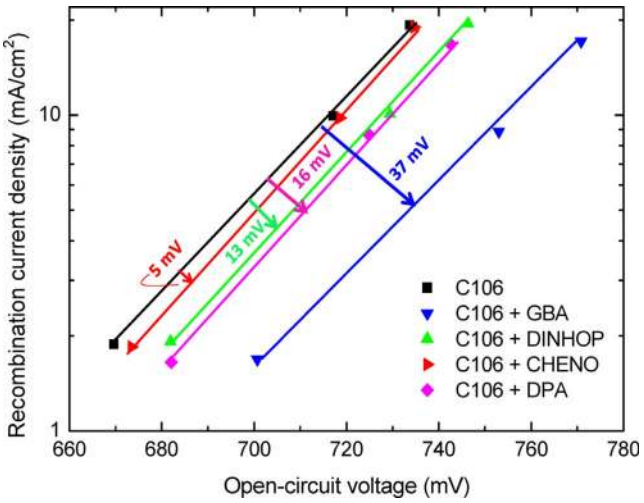

Figure 5. Recombination current density (J_R) as a function of the open-circuit voltage for C106 and co-sensitized DSSCs. The arrows and the corresponding numbers represent shifts of V_{OC} for any given J_R.

shows the J_{SC}, otherwise mentioned as recombination current density, measured at different light bias against their respective open-circuit voltages. Regardless of the type of cells, the evolution is linear between the recombination current density (in exponential scale) and the open circuit voltage. The photo-anode sensitized along with an additive shows a very similar evolution with a comparable slope but shifted to higher open-circuit voltage. Cheno is the less shifted, only ca. 5 mV, confirming either the absence of cheno to the surface or to a minor extent, insufficient to show an effective blocking character. The carboxy functional co-adsorbent exhibited a shift of 13 mV in the case of dinhop, 16 mV in the case of DPA and finally as high as 37 mV in the case of GBA. This latter shows the greatest passivating properties against electron recombination from the series. This result explains the reason why the cell photovoltage is improved by the utilization of GBA to this extent.

In the case of GBA, the negative dipole shift of trap states roughly equals the increase of V_{OC} but on other hand the −28 mV shift due to cheno is not reflected in the V_{OC}. From the above discussions, it can be concluded that neither GBA nor cheno acts as a blocking agents and in fact cheno, which is considered as a perfect co-adsorbent, is enhancing the recombination of photo generated electrons. If cheno is inert on the titania surface, a 28 mV increase in V_{OC} should have evidenced due to the band edge shift, but the increase observed is 5 mV and this result explains that this molecule is acting as an electron leak path. With phosphinic additive, the enhancement of V_{OC} is 8 mV higher compared to the up shift of the trap energy levels. Despite a 50 mV positive shift of surface traps for DPA, the open-circuit potential is increased by around 16 mV, at any given charge density indicating overall increase of 66 mV. In terms of blocking the back reaction phosphonic acid additive is the best. In addition to the variation of V_{OC} due to the surface electronic structure modification and the blocking effect, an increase in the short-circuit density is observed at low levels of addition of carboxy and phosphinic acid functionals, despite unmodified dye uptake. This probably explains the ability of these molecules to align the dyes on the surface in a way to favor excellent electron injection from their excited states. The IPCE increase shown in Figure 2 cannot come from enhanced absorption as the dye uptake is not increased in any of cases of co-adsorbed samples, and this increase can be purely ascribed to the "equilibrium" orientation of dye molecules. However further study is needed to understand this property clearly. Another property that has to be discussed is the de-aggregation of dyes due to the co-adsorbents. It is known that aggregates quench the photo excited electrons which will reduce the both the injection efficiency and the V_{OC}.[4c] In the case of GBA, as the V_{OC} increase was purely the band edge shift, no credits can be given to it for de-aggregation effect. In the rest other cases where recombination resistance comes into play, de-aggregation can also be a factor for higher V_{OC}. This factor can be separated only when the exact V_{OC} variation is calculated due to the blocking effect. The results still remain ambiguous to explain these hidden interconnected parameters.

3. Conclusions

In this work, we investigated the properties of carboxy- (GBA, Cheno), phosphinic- (dinhop) and phosphonic- (DPA) based functional molecules to co-adsorbe along the absorber in dye-sensitized solar cells to enhance the photovoltaic performances of already topmost devices. In conjunction with the ruthenium(II) polypyridil-based C106 complex, an optimized concentration of GBA or dinhop has enabled reaching a record power conversion efficiency of 11.0% by comparison to 10.6% for the reference device or for the 1:1 cheno-to-dye ratio typically utilized in the literature. Our results showed that depending on the type of additive and its concentration, one can enhance

the short-circuit current density without modifying the open-circuit voltage (GBA 6:1 and dinhop 2:1 ratio) thanks to π-π stacked aggregates breaking reducing self-quenching of the dye and improving electron injection and *vice-et-versa* for greater concentration (dinhop 0.5:1 ratio) owing to a reduction of recombination between TiO_2 and tri-iodide. Regardless of their concentration, we demonstrated that GBA, dinhop and DPA are truly co-adsorbents based on ATR-TF-IR spectroscopy. The case of cheno is more delicate since we concluded that the cheno is not, or to a very low extent (lower than FT-IR sensitiveness), a co-adsorbent with ruthenium dyes at a dye-to-co-adsorbent ratio of 0.5:1. This work discusses the role of the co-adsorbents on the dye uptake, band edge shift and ability to hamper the back reaction with tri-iodide. Based on our results, DPA and dinhop are showed to block the photoelectron recombination with tri-iodide. This is in contrast with the GBA which seems not having any passivating properties and to the controversial cheno which seems even accelerating the interfacial recombination. Neale et al. however, reported the similar effect as we observed where the band edge is shifted negative and rate of recombination is increased.[6a] The latter parameter dominates the former in determining the open-circuit potential of the device. The effect of de-aggregation of dye molecules and the change in mode of dye adsorption due to these co-adsorbents have to be clarified yet.

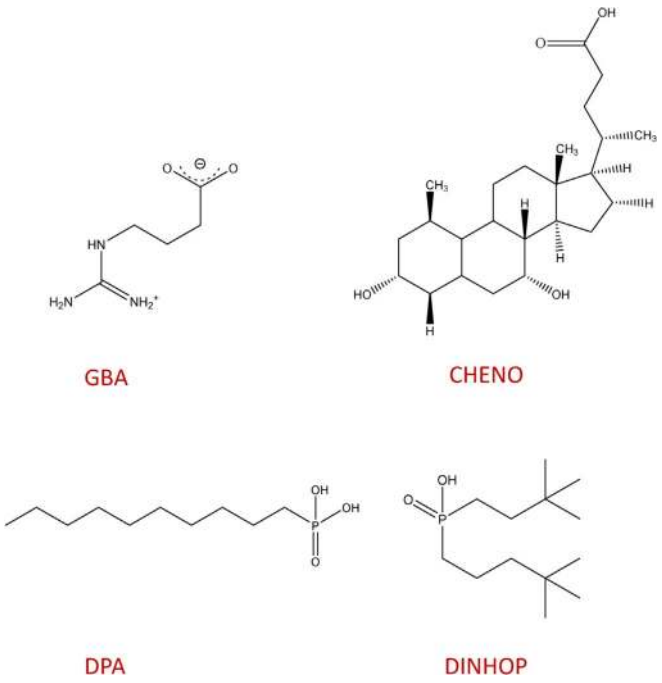

Scheme 1. Molecular structures of different co-adsorbents.

Experimental Section

Reagents and Chemicals

All the chemicals and solvents are puriss grade and were used as received. Di-methyl formamide (DMF), tert-butanol and acetonitrile were obtained from Fluka. The co-adsorbents 4-guanidino butyric acid (GBA), chenodeoxycholic acid (Cheno), and 1-dodecyl phosphonic acid (DPA) were received from Merck. The dineohexyl phosphinic acid (dinhop) was synthesized as described in the literature [6e]. One proton analogs of GBA zwitterion (GBA.HCl) and DPA (DPA.TBA) were made by adding either one equivalent of hydrochloric acid in the solution for GBA or neutralizing with one equivalent of hydroxyl group using tetrabutyl ammonium hydroxide for DPA. The chemical structures of different co-adsorbents are shown in Scheme 1. The mesoscopic nanocrystalline titanium dioxide films were prepared by screen-printing using a commercially available paste (Dyesol-DSL 30 NRD-T).

Preparation of Dye and Dye-Co-Adsorbent Solutions

For all the photovoltaic and characterization studies described herein, 300 μmol L^{-1} of C106 dye solution with/without co-adsorbents (namely, GBA, GBA.HCl, cheno, dinhop, DPA or DPA.TBA) were used in the solvent mixture of 10% DMF +90% 1:1 in volume ratio of acetonitrile and tert-butanol. Five different dye to co-adsorbent molar ratio (D:C) have been investigated, from 6:1, 4:1, 2:1, 1:1 and 0.5:1.

Device Fabrication

NSG10 (Nippon Sheet Glass, Japan) FTO glass was washed in water and ethanol followed by 30 min ultrasonic cleaning in Deconnex solution. The TCO was then thermally treated at 520 °C for 30 min to remove organic contaminants on the surface. The cleaned substrate was chemically treated in a 40 mM aqueous $TiCl_4$ solution for 30 min at 75 °C. After this step, the nano-crystalline TiO_2 films were deposited by screen-printing. The porogen was thermally removed by following a series of sintering steps corresponding to the subsequent plateau of degradation of the ethyl cellulose (325 °C for 5 min with 15 min ramp time, 375 °C for 5 min with 5 min ramp time, 450 °C for 15 min with 5 min ramp time and 500 °C for 15 min with 5 min ramp time). Before sensitization, the films sustained a last thermal treatment at 500 °C for 30 min to remove the surface contaminants on TiO_2's surface. The sensitization was carried out for 14 hours at 25 °C in darkness. The sensitized photoanode is then washed in acetonitrile to remove the loosely bounded dye molecules before cell assembly or characterization by FT-IR. For counter electrode, Pt coated TEC7 FTO (purchased from Solaronix, Switzerland) was used. Pt deposition was achieved by thermal decomposition at 410 °C for 20 min of the 2 mM H_2PtCl_6 ethanolic solution drop casted prior onto the conductive glass. The two electrodes were sealed using a 25 μm thick surlyn polymer film. The electrolyte is composed of 1 mol L^{-1} of 1–3 dimethyl imidazolium iodide (DMII), 50 mmol L^{-1} of LiI, 30 mmol L^{-1} of I_2, 0.5 mol L^{-1} of tert-butylpyridine and 0.1 mol L^{-1} of guanidinium thiocyanate (GuNCS) in a solvent mixture (85/ 15 by v.) of acetonitrile and valeronitrile. The electrolyte is injected into the device by vacuum backfilling technique through a hole sand blasted at the side of the counter electrode. Reproducibility on the device efficiency is in the range of +/−0.10% in the total power conversion efficiency.

Photovoltaic Characterization

A 450 W xenon lamp (Oriel, USA) was used as a light source. The spectral output of the lamp was filtered using a Schott K113 Tempax sunlight filter (Präzisions Glas & Optik GmbH, Germany) to reduce the mismatch between the simulated and actual solar spectrum to less than 4%. Keithley model 2400 digital source meter (Keithley, USA) was used for data acquisition. The photo-active area

of 0.159 cm^2 was defined by a black metal mask. Incident photon-to-current conversion efficiency measurements were carried out from a homemade setup using a Gemini-180 double monochromator Jobin Yvon Ltd., powered by a 300 W xenon light source (ILC Technology, USA). A white light bias was superimposed to the monochromatic light using 10 $mW\,cm^{-2}$ white LEDs. Monochromatic light was chopped at 1 Hz frequency. Devices were reproduced at least 5 times. Reproducibility on cell efficiencies is in the range or less than 0.1% with respect to the value of efficiency.

Dye Loading Determination

The dye loading was determined on 9 μm thick transparent TiO_2 films by desorbing the dye in DMF containing tetrabutyl ammonium hydroxide. The film area was 0.283 cm^2. The absorbance of the resulting solution was measured by UV/Vis spectrophotometry (model: Hewlett Packard 8452A diode array spectrophotometer) at MLCT wavelength. The concentration was determined using Beer–Lambert law ($\varepsilon_{C106} = 18\,700\ M^{-1}\,cm^{-1}$).[7d]

ATR-FTIR Spectroscopy

ATR-FTIR spectra were measured using a FTS 7000 FTIR spectrometer (Digilab, USA) fitted with a "Golden Gate" diamond anvil ATR accessory which is constantly purged with dry nitrogen gas. The dye sensitized films with/without co-adsorbents are washed in acetonitrile and dried before any measurements. The spectra were derived from 64 scans at a resolution of 2 cm^{-1}.

Charge Extraction Measurements

The density and distribution of surface trap states were estimated from the number of extracted charges obtained at different light intensities, from 1.5 to 0.16 sun. The source of photon used was an array of white LEDs fitted with the cooling system to ensure uniform emission spectrum. The charge extraction is carried out by turning off the LED illumination source while simultaneously switching the cell from open to short-circuit. The data are collected by a Keithley 2400 source meter. From the number of charges extracted for different light intensities, the density of surface trap states (DOS) are calculated using Equation (1):

$$\mathrm{DOS} = (6.24 \times 10^{18})\ C/d(1-p)$$

where C is the capacitance measured, and d and p are the film thickness and porosity, respectively.[13]

Supporting Information: A table of photovoltaic parameters for one-proton analogs of guanidino butyric acid and dodecyl phosphonic acid, and ATR-FTIR spectra of chenodeoxycholic acid adsorbed on the titania surface are available free of charge in the Supporting Information.

Acknowledgements

We thank Prof. Peng Wang, Chinese Academy of Sciences for providing us the C106 dye. The authors acknowledge financial support of this work by EU FP7 project "ORION" grant agreement number NMP-229036.

Conflict of interest

The authors declare no conflict of interest.

Keywords: co-adsorbents · dye-sensitized solar cells · interfaces · photovoltaics · titanium dioxide

[1] S. Namba, Y. Hishiki, *J. Phys. Chem.* **1965**, *69*, 774–779.
[2] a) H. Meier, *J. Phys. Chem.* **1965**, *69*, 719–729; b) E. Inoue, T. Yamaguchi, *J. Chem. Soc. Jpn.* **1963**, *36*, 1573–1577; c) E. Inoue, H. Kokado, T. Yamaguchi, *J. Phys. Chem.* **1965**, *69*, 767–774.
[3] R. C. Nelson, *J. Phys. Chem.* **1965**, *69*, 714–718.
[4] a) E. Lendvay, *J. Phys. Chem.* **1965**, *69*, 738–744; b) A. Terenin, I. Akimov, *J. Phys. Chem.* **1965**, *69*, 730–738; c) J. Bourdon, *J. Phys. Chem.* **1965**, *69*, 705–713.
[5] a) B. O'Regan, M. Grätzel, *Nature* **1991**, *353*, 737; b) M. Grätzel, *Inorg. Chem.* **2005**, *44*, 6841; c) M. Grätzel, *Nature* **2001**, *414*, 338; d) M. Grätzel, *Acc. Chem. Res.* **2009**, *42*, 1788.
[6] a) N. R. Neale, N. Kopidakis, J. van de Lagemaat, M. Grätzel, A. J. Frank, *J. Phys. Chem. B* **2005**, *109*, 23183–23189; b) J.-H. Yum, S.-R. Jang, R. Humphry-Baker, M. Grätzel, J.-J. Cid, T. Torres, M. K. Nazeeruddin, *Langmuir* **2008**, *24*, 5636; c) T. Marinado, M. Hahlin, et al., *J. Phys. Chem. C* **2010**, *114*, 11903; d) M. Wang, C. Grätzel, S.-J. Moon, R. Humphry-Baker, N. Rossier-Iten, S. M. Zakeeruddin, M. Gratzel, *Adv. Funct. Mater.* **2009**, *19*, 2163; e) M. Wang, X. Li, H. Lin, P. Péchy, S. M. Zakeeruddin, M. Grätzel, *Dalton Trans.* **2009**, 10015; f) P. Wang, S. M. Zakeeruddin, R. Humphry-Baker, J. E. Moser, M. Grätzel, *Adv. Mater.* **2003**, *15*, 2101; g) X. Li, H. Lin, S. M. Zakeeruddin, M. Gratzel, J. Li, *Chem. Lett.* **2009**, *38*, 322; h) Z. Zhang, N. Evans, S. M. Zakeeruddin, R. Humphry-Baker, M. Grätzel, *J. Phys. Chem. C* **2007**, *111*, 398; i) Z. Zhang, S. M. Zakeeruddin, B. O'Regan, R. Humphry-Baker, M. Gratzel, *J. Phys. Chem. B* **2005**, *109*, 21818; j) M. Flasque, A. N. Van Nhien, J. Swiatowska, A. Seyeux, C. Davoisne, F. Sauvage, *ChemPhysChem* **2014**, *15*, 1126–1137; k) M. Flasque, A. N. Van Nhien, D. Moia, P. R. F. Barnes, F. Sauvage, *J. Phys. Chem. C* **2016**, *120*, 18991–19998.
[7] a) Y. Chiba, A. Islam, Y. Watanabe, R. Komiya, N. Koide, L. Han, *Jpn. J. Appl. Phys.* **2006**, *45*, L638; b) Y. Chiba, A. Islam, R. Komiya, N. Koide, L. Han, *Appl. Phys. Lett.* **2006**, *88*, 223505–1; c) F. Gao, Y. Wang, D. Shi, J. Zhang, M. Wang, X. Jing, R. Humphry-Baker, P. Wang, S. M. Zakeeruddin, M. Grätzel, *J. Am. Chem. Soc.* **2008**, *130*, 10720; d) Y. Cao, Y. Bai, Q. Yu, Y. Cheng, S. Liu, D. Shi, F. Gao, P. Wang, *J. Phys. Chem. C* **2009**, *113*, 6290.
[8] F. Sauvage, J. D. Decoppet, M. Zhang, S. M. Zakeeruddin, P. Comte, M. K. Nazeeruddin, P. Wang, M. Graetzel, *J. Am. Chem. Soc.* **2011**, *133*, 9304–9310.
[9] J.-H. Yum, P. Walter, S. Huber, D. Rentsch, T. Geiger, F. Nüesch, F. De Angelis, M. Grätzel, M. K. Nazeeruddin, *J. Am. Chem. Soc.* **2007**, *129*, 10320.
[10] L. M. Peter, *Phys. Chem. Chem. Phys.* **2007**, *9*, 2630.
[11] a) R. J. Hamers, *Annu. Rev. Anal. Chem.* **2008**, *1*, 707; b) L. Zuppiroli, L. Si-Ahmed, K. Kamaras, F. Nüesch, M. N. Bussac, D. Ades, A. Siove, E. Moons, M. Grätzel, *Eur. Phys. J. B* **1999**, *11*, 505; c) A. Vilan, J. Ghabboun, D. Cahen, *J. Phys. Chem. B* **2003**, *107*, 6360; d) G. Schlichthörl, S. Y. Huang, J. Sprague, A. J. Frank, *J. Phys. Chem. B* **1997**, *101*, 8141; e) S. Rühle, M. Greenshtein, S. G. Chen, A. Merson, H. Pizem, C. S. Sukenik, D. Cahen, A. Zaban, *J. Phys. Chem. B* **2005**, *109*, 18907.
[12] M. K. Nazeeruddin, S. M. Zakeeruddin, R. Humphry-Baker, M. Jirousek, P. Liska, N. Vlachopoulos, V. Shklover, C. H. Fischer, M. Grätzel, *Inorg. Chem.* **1999**, *38*, 6298–6305.
[13] N. W. Duffy, L. M. Peter, R. M. G. Rajapakse, K. G. U. Wijayantha, *Electrochem. Commun.* **2000**, *2*, 658.

Manuscript received: May 4, 2017
Revised manuscript received: June 26, 2017
Version of record online: September 7, 2017